Volume 11
Number 1
January 2026
Pages 1–316

Nanoscale Horizons

The home for rapid reports of exceptional significance in nanoscience and nanotechnology

rsc.li/nanoscale-horizons

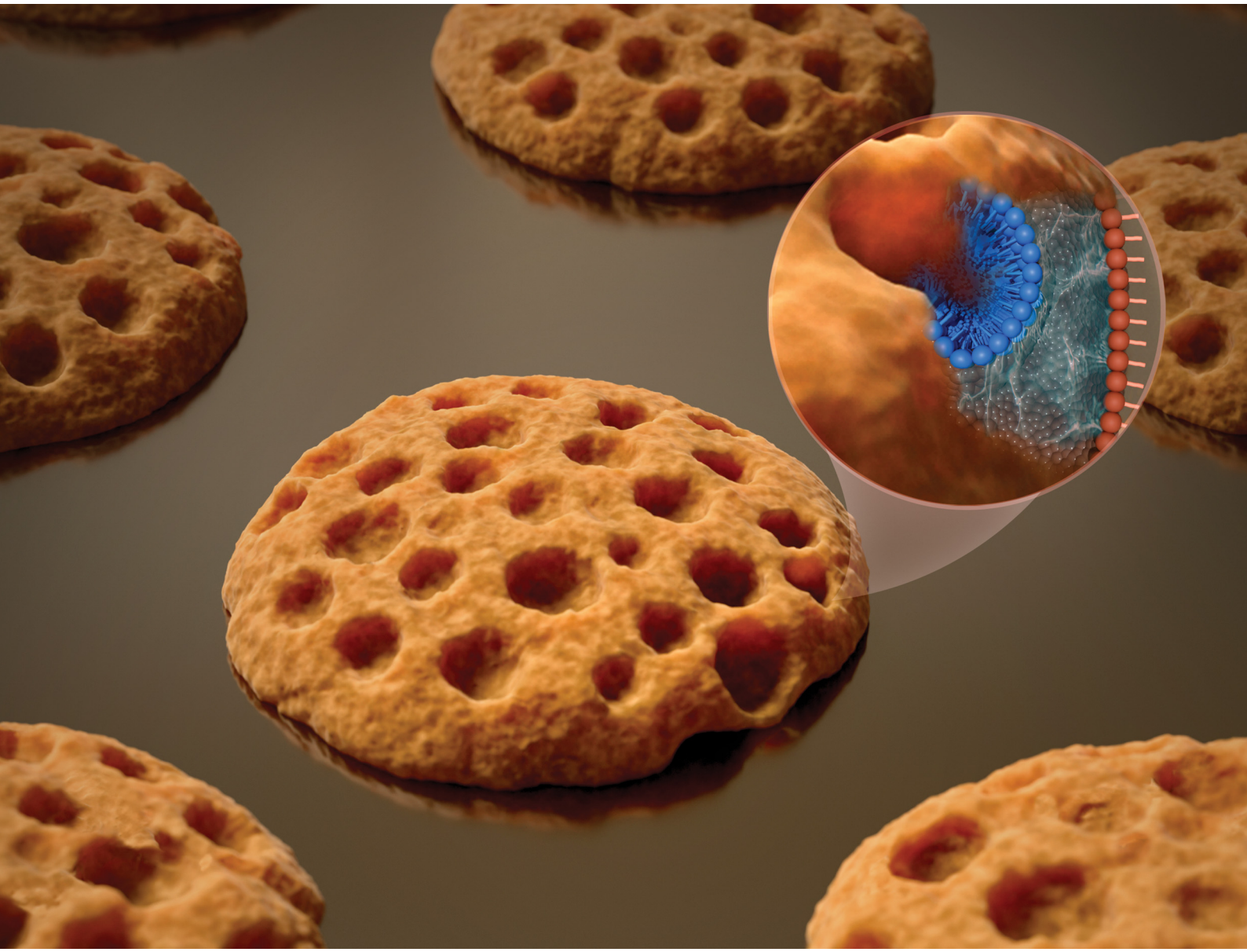

ISSN 2055-6756

ROYAL SOCIETY OF CHEMISTRY

COMMUNICATION
Emilio M. Pérez, Mark W. Rutland *et al.*
Self-assembly of microscale architectures with nanoscale inclusions

NCNST

Nanoscale Horizons

ROYAL SOCIETY OF CHEMISTRY

COMMUNICATION

View Article Online
View Journal | View Issue

Cite this: *Nanoscale Horiz.*, 2026, **11**, 157

Received 20th May 2025,
Accepted 29th September 2025

DOI: 10.1039/d5nh00356c

rsc.li/nanoscale-horizons

Self-assembly of microscale architectures with nanoscale inclusions

Alicia Naranjo, [a] Marine Batista, [b] Emilio M. Pérez *[a] and Mark W. Rutland *[bcde]

We hypothesise that the recent discovery of nanodomains at the air–water interface can be leveraged to nano-functionalize surfaces through casting with incorporated functional species. The interfacial self-assembly of the amphiphilic molecules, 18-methyleicosanoic acid 18-MEA and 4-(tetradecyl)benzene diazonium tetrafluoroborate TDDS, at the air–water interface and cast on silicon wafer has been investigated using Langmuir–Blodgett (LB) techniques and atomic force microscopy. The impact of composition and surface pressure (SP) on the formation of nanodomains and microstructures was examined. TDDS (which can be used to modify the electronic structure of graphene) behaves as a co-surfactant in the 18-MEA film at low concentrations, facilitating the formation of homogeneous nanodomains with functional capacity. At higher TDDS concentrations, there is evidence for phase separation in the domains, and the TDDS furthermore partitions to the aqueous phase at higher pressures. By manipulating the 18-MEA:TDDS ratio and SP, regular nano-patterns can be transitioned into novel 2D structures reminiscent of 3D water-in-oil-in-water (W/O/W) analogues ("cookie systems"), offering a versatile strategy for designing nanoarchitectures with potential applications in graphene patterning.

New concepts

We demonstrate a simple strategy to create functional nanostructures at the air–water interface by co-assembling an amphiphilic fatty acid (18-MEA) with a diazonium compound (TDDS), and transferring the resulting films onto solid substrates. This work shows that nanodomains emerging spontaneously at the interface can be tuned by adjusting the molecular composition and surface pressure, offering a route to controlled nano-patterning without the need for lithography. The use of TDDS, which can covalently modify carbon-based materials such as graphene and MoS_2, adds a chemical functionality to the nanodomains, enabling further modification after film transfer. Unlike most studies that rely on single-component films or post-assembly patterning, our approach exploits co-surfactant behaviour and interfacial dynamics to guide structure formation directly during film assembly. We also observe a transition from regular nanodomains to complex, periodic 2D patterns resembling 3D water-in-oil-in-water systems ("cookie structures"), suggesting new possibilities for designing hybrid interfacial architectures. This work provides mechanistic insight into interfacial phase behaviour in mixed amphiphilic films and opens up new pathways for creating chemically functionalised nanostructures with potential use in soft patterning, sensing, or surface engineering of 2D materials.

Emilio M. Pérez

Congratulations to Nanoscale Horizons for completing ten turns around the sun! In its role as the flagship journal of the Nanoscale family, it continues to provide a perfect venue for publication of results at the forefront of nanoscience. It is always a pleasure to contribute to the journal, both as an author and as a referee. For this special issue, we joined forces with Mark Rutland to bring some nano-cookies to the party. Here's to many more to come!

Introduction

The air–water interface is ideal for systematic investigations of the self-assembly of insoluble, amphiphilic molecules.[1] The dual nature of these compounds—containing both hydrophilic

[a] *IMDEA Nanociencia, C/Faraday 9, Ciudad Universitaria de Cantoblanco, 28049 Madrid, Spain. E-mail: emilio.perez@imdea.org*
[b] *KTH Royal Institute of Technology, Department of Chemistry, Stockholm SE-100 44, Sweden. E-mail: mark@kth.se*
[c] *School of Chemistry, University of New South Wales, Sydney 2052, Australia*
[d] *Laboratoire de Tribologie et Dynamique des Systèmes, École Centrale de Lyon, Lyon 69130, France*
[e] *Bioeconomy and Health, Materials and Surface Design, RISE Research Institutes of Sweden, Stockholm, Sweden*

and hydrophobic moieties—enables them to spontaneously organize at interfaces into several structures, such as mono- or bi-layers, in order to minimize energy and achieve thermodynamic stability.[2,3] The Langmuir–Blodgett (LB) method enables precise control over such assemblies by mechanical manipulation at the air–water interface, offering greater molecular-level control for the precise formation of mono- and multilayers. This technique also provides milder processing conditions, simplicity, cost-effectiveness, versatility, and environmentally friendly processes, making it highly attractive for a wide range of applications in various fields, including electronics,[4] optics,[5] sensors[6,7] and biomaterials.[8] In this context, LB techniques have also been applied to deposit nanoparticles, enabling the fabrication of novel nanocomposite films,[9] the precise functionalization of surfaces[10] at the molecular level, and the development of organic electronic devices,[11] owing to their ability to create highly ordered molecular structures. These nanostructures depend on the packing parameter, which determines the size and shape of the various assemblies within mesophases and aids in understanding the self-assembly of insoluble monolayers.[12] Furthermore, building nanoarchitectures from two-component monolayers must consider the monolayer composition and intermolecular forces within it.[13,14] The miscibility of the components and the free-energy of mixing for the 2D-solution can define the behavior of one component relative to the other, thereby significantly influencing the resultant monolayer.

It has recently been reported[15,16] that the use of branched fatty acids causes the water interface to be buckled by the formation of self-assembly nanodomains. This in turn enables surface patterning of the transferred films—for example, using 18-methyleicosanoic acid (18-MEA). Non-branched fatty acids lead to completely flat surfaces, whereas the presence of alkyl branches results in the formation of surface domains, the size and curvature of which depend on the position of the branches.[17] Moreover, combining branched and non-branched fatty acids in different ratios allows systematic tuning of the dimensions.

Incorporating functional molecules into this bottom-up approach enables their controlled and systematic placement on different nanomaterials. To explore this potential, we investigate whether the nanodomains formed by branched fatty acids could act as templates to organize reactive amphiphilic molecules within thin films—an important step toward precise surface patterning and nanoscale chemical modification.

As a model system, we incorporated a para-substituted diazonium salt, 4-(tetradecyl)benzene diazonium tetrafluoroborate (TDDS), into the nanodomains described above.[15,16] TDDS was specifically chosen due to its long alkyl chain, which enhances its compatibility with the hydrophobic environment of the monolayer, and its reactive diazonium functionality, which opens the door for future chemical modifications.

Although functionalization of materials like graphene[18,19] represents a long-term motivation—given its unique physicochemical properties[20–22] and emerging role in nanotechnology—the current study is focused on understanding the interfacial organization and structural properties of these hybrid monolayers.

Here, we report the serendipitous discovery of the complex hierarchical self-assembled nanoarchitectures formed by the coexistence of 18-MEA (a fatty acid) and TDDS, offering a promising foundation for bottom-up approaches in nanofabrication and surface chemistry.

Results and discussion

As a calibration, the deposition of pure 18-MEA from the air–water interface onto a silicon substrate was carried out using the LB technique at a surface pressure (SP) of 20 mN m^{-1} (Fig. 1a). As previously reported, pure 18-MEA exhibited monodisperse nanodomains (Fig. 1b).[16] Subsequently, a homogeneous mixture of 18-MEA and TDDS (see SI, Fig. S1 and S2 for additional details) in a 90 : 10 mol% ratio was prepared as described in the Experimental methods section, and deposited under the same conditions at a SP of 20 mN m^{-1} (Fig. 1c).

The resulting domains are relatively monodispersed, indicative of a thermodynamic minimum in the self-assembly process, and are significantly larger than those observed in Fig. 1b. This observation is consistent with a reduced curvature associated with the increased proportion of the unbranched TDDS component. Consequently, this results in domains with a larger radius, and lower curvature, at the air–water interface, hence the elongation and correspondingly larger domains in the AFM images. Corresponding height images are provided in Fig. S3 of the SI. This necessarily implies that a substantial portion of the TDDS is homogeneously distributed within the domains, suggesting solubilization in the major component, 18-MEA. A close inspection of the isotherm in Fig. 2 reveals variations in the gradient, which may imply the possibility of structural differences depending on the deposition pressure, as further discussed below.

To comprehensively investigate the joint behaviour of these two organic compounds, a systematic series of isotherms at the

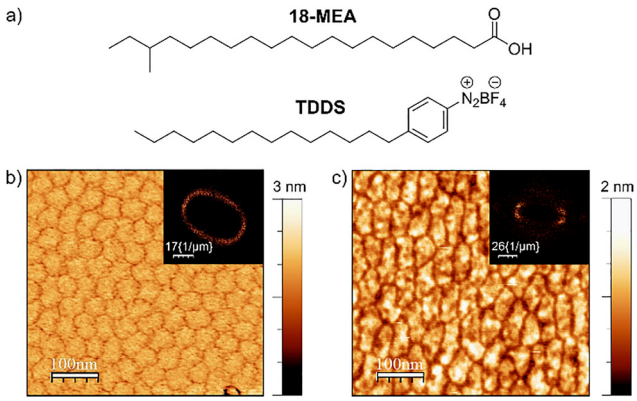

Fig. 1 (a) Molecular structures of the organic compounds: 18-methyleicosanoic acid (18-MEA, top) and the diazonium salt TDDS (bottom); (b) AFM height image of monodispersed nanodomains of pure 18-MEA deposited at 20 mN m^{-1}; (c) AFM height image of a mixed monolayer of 18-MEA:TDDS (90 : 10 mol%) deposited at 20 mN m^{-1}. Scan area: 500 × 500 nm. Insets in the top right corners show the corresponding Fourier transforms.

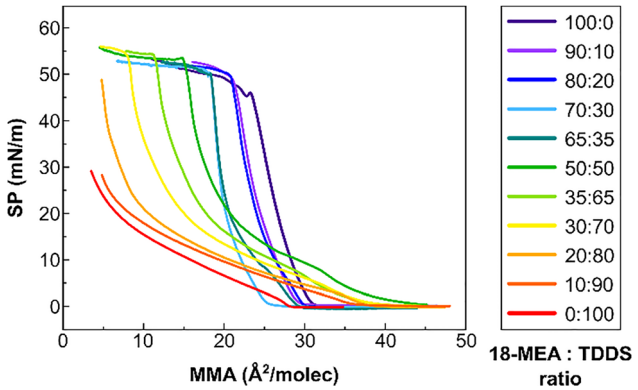

Fig. 2 Isotherm trend for different 18-MEA:TDDS molar ratios. Surface pressure is plotted against the mean molecular area, assuming a 2D interface.

water–air interface were recorded for different 18-MEA:TDDS molar ratios (Fig. 2): 100 : 0, 90 : 10, 80 : 20, 70 : 30, 65 : 35, 50 : 50, 35 : 65, 30 : 70, 20 : 80, and 0 : 100. A clear trend emerges, allowing for the identification of three distinct regimes based on the shape of the isotherms: (i) fatty acid-like behaviour (100 : 0 to 70 : 30), (ii) a phase transition regime (65 : 35 to 30 : 70), and (iii) a regime dominated by solubilization of TDDS molecules (20 : 80 to 0 : 100). The rationale behind these assignments is discussed in detail below.

In the fatty acid-like regime (100 : 0 to 70 : 30 mol%) the lift-off of the surface pressure (SP) occurred at a mean molecular area (MMA) of approximately 25–32 Å^2. It is important to note that MMA is classically calculated under the assumption of a flat interface defined by the barrier positions and therefore does not accurately reflect the true molecular area within the curved nanodomains SP $>$ 0 mN m^{-1}.[23] The MMA decreases slightly with increasing TDDS concentration within this regime, which is consistent with the absence of branching. However, caution should be exercised in interpreting these changes, as minor variations—on the order of a few Å^2—may also arise from experimental uncertainties in the estimation of the number of molecules deposited (see Materials and methods). The isotherm subsequently increases until film collapse, occurring at a nearly constant pressure of 46–52 mN m^{-1}. This behaviour aligns well with previously reported isotherms of pure fatty acids, suggesting a single-component system exhibiting characteristic nanodomain formation.[15,16,23] Within this regime, TDDS appears to behave as a dilute additive within the surface film.

At intermediate TDDS mole fractions (65 : 35 to 30 : 70 mol%), a distinct behaviour emerges—referred to here as the phase transition regime. This regime is characterized by the appearance of a shoulder in the isotherms at approximately 10 mN m^{-1}. As the TDDS content increases, the lift-off area shifts to significantly larger values (*ca.* 35–40 Å^2), which are indicative of a liquid-expanded phase. Although these samples collapse at the same pressure as those in the fatty acid-like regime, the observed MMA at collapse is unrealistically low if all molecules are assumed to remain in the film. However, the collapse areas are consistent with the amounts of fatty acids in the original films, or at least with a low concentration of TDDS. These observations suggest that, at low surface pressures, the film behaves as a mixed monolayer of TDDS and 18-MEA, but as the pressure increases, the more soluble TDDS is progressively excluded. Ultimately, the film collapses at a composition and area characteristic of the fatty acid-dominated regime.

Finally, the third regime, referred to as "solubilized molecules" (20 : 80 to 0 : 100 mol%), is characterized by the absence of collapse and an extremely low slope in the isotherm. This regime can be considered as an extension of the pressure-induced exclusion behaviour observed in the second regime, but with a sufficiently diluted fatty acid composition such that there is not enough barrier range to reach collapse pressure. Pure TDDS, on the other hand, can achieve a pressure of approximately 30 mN m^{-1}; however, the molecular area per molecule suggests that less than a quarter of the molecules remain on the surface (assuming a cross-sectional area of 20 Å^2 per molecule and a flat surface).

Based on the behaviour observed in the different isotherms, two new samples were selected for a more detailed study and comparison with the 90 : 10 mol% sample (chosen due to its similarity to previous studies). These samples were deposited at different surface pressures to investigate domain formation and packing. The selected samples were 65 : 35 mol% and 35 : 65 mol%, both within the phase transition regime, with the latter being very close to the behaviour of "solubilized molecules". Given the initial goal of this project, which was to achieve nanopatterns containing an active component, mixtures with a higher fraction of TDDS (which is partially soluble in water) were not considered viable.

Surprisingly, no nanodomains were obtained for the 65 : 35 mol% mixture when deposition was performed at 20 mN m^{-1} or higher (including 35 mN m^{-1}, close to collapse). Instead, circular particles with varying lateral sizes were observed across the surface, which were transferred onto the silicon substrate (see SI, Fig. S4 for images). The particles, with a height of 16 $\pm$ 8 nm, appeared to be systematically distributed, with some vestigial hexagonal packing remaining, except in areas where larger particles (83 $\pm$ 17 nm in height) were surrounded by bare regions—suggesting aggregation. This observation implies that, in the presence of higher amounts of TDDS, when high surface pressure is applied, molecules tend to partially dissolve in the subphase and coalesce into circular macrodomains, probably during deposition onto the substrate.

However, experiments performed at low surface pressure, below the shoulder observed in Fig. 3a) at around 10 mN m^{-1}, showed very different, novel morphologies. Such a shoulder is not observed for pure 18-MEA (Fig. 3a) or low fractions of TDDS (Fig. 2). This change in slope indicates that different structures can be expected on either side of it, with expulsion and possibly coalescence at higher SP.

Deposition at 5 mN m^{-1}, resulted in novel morphologies of the deposited films: microdomains containing nanodomains. As shown in Fig. 3b, rounded domains encapsulating circular holes were observed after deposition, reminiscent of a chocolate-chip cookie structure. Fig. 3c and d show zoomed-out

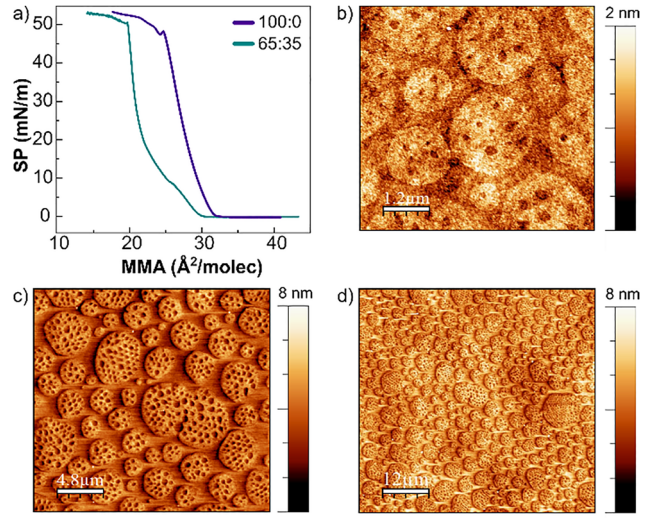

Fig. 3 (a) Isotherm profile of the 65 : 35 mol% sample; (b)–(d) AFM height images of 65 : 35 mol% at a surface pressure of 5 mN m^{-1}. Scanning size of 6 × 6 µm, 24 × 24 µm and 60 × 60 µm, respectively.

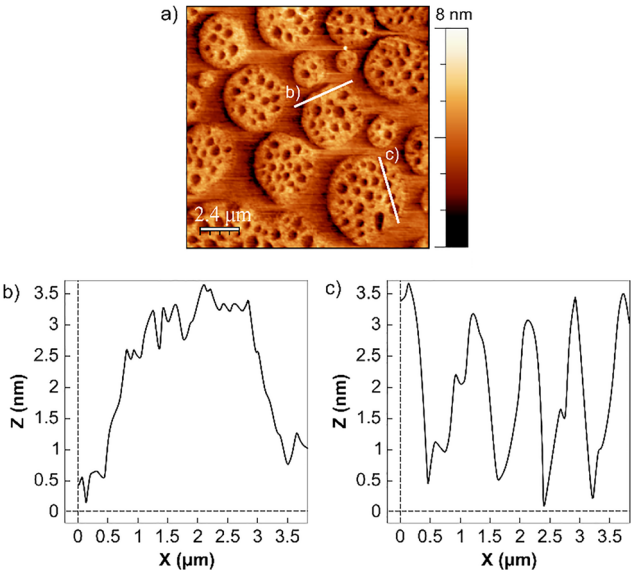

Fig. 4 (a) AFM height image from deposition of 65 : 35 mol% 18-MEA:TDDS at SP of 20 mN m^{-1}, showing line cuts for (b) and (c). Scanning size of 12 × 12 µm; (b) height profile of the cookie surface and (c) height profile of four empty-holes.

images of the same substrate. The patterned surface was homogeneous, with rounded domains measuring 2.6 ± 1.1 µm, and circular encapsulated holes with a diameter of 228 ± 65 nm. Corresponding AFM phase images are provided in the SI, Fig. S5. These domains suggest the spontaneous formation of a two-dimensional double emulsion-like architecture (presumably W/O/W, where the "water" phase is TDDS rich and the "oily" phase is 18-MEA rich), due to the higher content of TDDS relative to 18-MEA, which is nonetheless still low enough to allow domain formation.

In this context, we propose that the rounded domains are almost entirely composed of 18-MEA, with TDDS dissolved within it, acting as a cosurfactant. It is likely that the holes are the result of phase separation within the domains and subsequent dissolution of TDDS, but whether this occurs at the water-air interface, or because of deposition is impossible to determine. (Alternatively, but less probably, they may be the result of a significant change in area of the domain as it is deposited on the substrate.) The thickness of the cookie matrix structure is 2.6 ± 0.3 nm, measured both at the edges of the cookie and inside the holes, which appear to be empty (Fig. 4).

To further confirm this behaviour, depositions immediately below (7.5 mN m^{-1}) and above (10 mN m^{-1}) the shoulder pressure were also performed. At 7.5 mN m^{-1}, the cookie-like architecture was maintained, with the appearance of a mesh-like network between the rounded domains. This suggested that 18-MEA molecules could reaggregate into monodispersed, ellipse-like domains. At 10 mN m^{-1}, the domains began to deform, with some collapsing into neighbouring domains, and smaller circular particles appeared at the junction points. This behaviour indicated that as the transition phase approached, TDDS may have been released from the 18-MEA moiety, promoting the crystallization of smaller circular TDDS droplets. At 12.5 mN m^{-1}, the architecture was completely lost, and a continuous amorphous monolayer with circular particles was observed, like those seen at 10 mN m^{-1}. For a more detailed analysis, including AFM images of the depositions at 7.5, 10, and 12.5 mN m^{-1}, refer to the SI, Fig. S6–S9.

In the concentration regime where TDDS is highest and is expelled from the film at the water air interface (regime (iii) in Fig. 2), the deposited films have rather interesting morphologies involving circular particles but are difficult to interpret and are unlikely to attain any practical applications. This regime is thus fully addressed only in the SI (Fig. S10, S11 and Fig. S12).

Experimental

Reagents and solvents

18-Methyleicosanoic acid (18-MEA, >99% GC with approximately 1% of ethanol as stabiliser) was brought from Larodan and used as received. 4-Tetradecylaniline (97%) was brought from Sigma Aldrich and used as a precursor on the synthesis of 4-(tetradecyl) benzene diazonium tetrafluoroborate (TDDS). Sodium hydroxide (NaOH), sodium chloride (NaCl) and sodium bicarbonate ($NaHCO_3$) were also brought from Sigma Aldrich and used as provided.

All water used was supplied *via* a Milli-Q water purification system (Merck MilliPore). The system consistently monitors resistivity (above 18.2 MΩ) and total organic content (below 4 ppb).

Low roughness Si/SiO_2 wafers were purchased from Sil'Tronix ST and used after washes: through immersion in 5% chromosulfuric acid for 5 minutes followed by thorough rinsing with Milli-Q and drying with N_2 flow. Graphene substrates (supported on Si/SiO_2) were purchased from Graphenea and used as received.

Synthesis of 4-(tetradecyl) benzene diazonium tetrafluoroborate

The formation of the diazonium salt was performed as previously reported[24] by our group. Briefly, 4-tetradecylaniline (500 mg, 1.73 mmol, 1 eq.) and nitrosonium tetrafluoroborate (301 mg, 2.59 mmol, 1.5 eq.) were dissolved in 10 mL in two different Schlenk flasks under a nitrogen atmosphere and cooled to −40 °C. Then, 4-tetradecylaniline was slowly cannulated into the second solution and the mixture was stirred for 1 h. After that, the solutions were gradually warmed up to 0 °C during 2 h, while stirring. Finally, it was poured into cold Et_2O, and the yellow precipitate was then filtered, washed with Et_2O and dried under vacuum (89% yield). The solid was stored at −4 °C.

Solutions

Solutions of 1 mg mL 18-MEA and TDDS were prepared through dissolution in $CHCl_3$ at room temperature, and stored at −8 °C. The subphase was prepared by mixing 5 mL of 0.18 mM NaCl and 5 mL of 0.1 mM $NaHCO_3$ and buffered to pH = 10.0 with the addition of NaOH.

Langmuir–Blodgett isotherm and deposition

A KSV NIMA 5000 system (Biolin Scientific, Sweden) was used for isotherms and depositions. It was equipped with a PTFE (polytetrafluoroethylene) trough with hydrophilic POM (polyoxymethylene) barriers. Wilhelmy plates from lint free paper (Biolin Scientific) were used to monitor surface pressure to a certainty of ± 0.01 mN m^{-1}. The temperature of the subphase was set to 22.0 ± 0.1 °C. Monolayers were spreading on top of the subphase and $CHCl_3$ was allowed to evaporate for 10–15 minutes before starting the experiments. The barriers were then compressed by 3 mm/min for both isotherm and deposition experiments. Isotherms were analyzed in terms of surface pressure keeping the movement of the barriers constant. Depositions were performed on silicon wafers keeping the surface pressure constant at a different value (from 5 to 35 mN m^{-1}).

AFM

A Multimode Microscope LN (Bruker, United States) was used in tapping mode for imaging of deposited monolayers. Silicon cantilevers (HQ:NSC35/AL BS, MikroMasch, Switzerland) with a nominal radius of 8 nm were used. The nominal resonance frequency and force constant of the cantilevers were 150 kHz and 5.4 N m^{-1}, respectively. AFM images were analysed using the WsXM 5.0 software.

Conclusions

A range of well-defined self-assembled micropatterns with nano-sized inclusions can be achieved at the air–water interface and transferred onto silicon substrates using mixtures of TDDS and 18-MEA in water. The morphology of the patterns can be controlled through variations of the film composition and surface pressure.

TDDS appears to behave as a cosurfactant within the insoluble 18-MEA monolayer, particularly at low concentrations where it remains in the nanodomains. Thus, under these conditions, regular nanopatterns containing small amounts of the functionalizing agent can be systematically and reproducible deposited on a substrate where the 3D self-assembly nanodomains at the water surface are deposited intact.[14] This results in the homogeneous spatial arrangement of the functionalizing species. These complex and homogeneous structured films could in principle be reacted with a graphene substrate, achieving the goal of patterned covalent decoration.

As the TDDS proportion increases, the ability of TDDS to solubilize within the monolayer decreases. This reduction leads to two phenomena: Firstly, TDDS appears to be increasingly expelled from the interfacial film at higher pressures. Secondly TDDS appears to phase separate within domains in the interfacial film, which leads to the formation of micro-sized circular domains on the surface, containing circular holes of nanoscale dimensions. At even higher concentrations of TDDS, the domain structure becomes poorly defined.

At the intermediate TDDS levels, novel, apparently 2D microemulsion structures can be obtained. The formation of a W/O/W-like structure (cookie system), where TDDS remains incorporated as domains within the 18-MEA film is a novel observation which could be leveraged for other systems to deposit well defined 2D droplets of a lipid matrix incompatible species.

The approach provides a flexible strategy for patterning and creating diverse nanoarchitectures, as well as for delivering a functionalizing agent with regular spatial control. This approach thus shows particular promise for graphene patterning, where diazonium salts could be delivered at will and subsequently covalently anchored.

Author contributions

A. N. performed the experimental work, and contributed to data analysis, figure preparation, and manuscript writing. M. B. contributed to the experimental work. E. M. P. and M. W. R. conceived the idea, supervised the project and contributed to interpretation, manuscript writing and revision. All authors discussed the results and contributed to the final version of the manuscript.

Conflicts of interest

There are no conflicts to declare.

Data availability

Data for this article, including AFM and Langmuir isotherm data, are available at IMDEA Nanociencia Repository (**https://repositorio.imdeananociencia.org/home**) at **https://hdl.handle.net/20.500.12614/3978.**

Supplementary information (SI): synthetic and characterization details and supporting figures. See DOI: **https://doi.org/10.1039/d5nh00356c**.

Acknowledgements

MWR acknowledges support from the Swedish Research Council, VR, *via* grant VR2022-04614. The experiments were performed at 2MILab – the laboratory for Molecules and Materials at Interfaces, a KTH infrastructure. EMP acknowledges funding from the Ministerio de Ciencia, Innovación y Universidades (PID2023-152267NB-I00), and Comunidad de Madrid ''Materiales Disruptivos Bidimensionales (2D)'' (MAD2D-CM)-UAM and (MAD2D-CM)-IMDEA-NC funded by the Recovery, Transformation and Resilience Plan, and by NextGenerationEU from the European Union. IMDEA Nanoscience acknowledges support from the ''Severo Ochoa'' Programme for Centres of Excellence in R&D CEX2020-001039-S.

References

1 D. Lombardo, M. A. Kiselev, S. Magazù and P. Calandra, *Adv. Condens. Matter Phys.*, 2015, **1**, 151683.
2 S. Ghosh, A. Ray and N. Pramanik, *Biophys. Chem.*, 2020, **265**, 106429.
3 T. G. Barclay, K. Constantopoulos and J. Matisons, *Chem. Rev.*, 2014, **114**, 10217–10291.
4 A. E. Pérez Mendoza, A. Schmidt, E. Cavazzini Cesca, E. Westphal, J. P. M. Serbena, E. S. Orth, A. J. G. Zarbin and H. Winnischofer, *JCIS Open*, 2023, **9**, 100080.
5 Y. Li, C. Y. Wang and D. J. Qian, *Colloids Surf., A*, 2023, **673**, 131741.
6 C. Qian, R. Wang, M. Li, X. Li, B. Ge, Z. Bai and T. Jiao, *Colloids Surf., A*, 2021, **608**, 125616.
7 S. Choudhury, C. A. Betty, K. Bhattacharyya, V. Saxena and D. Bhattacharya, *ACS Appl. Mater. Interfaces*, 2016, **8**, 16997–17003.
8 S. Zhang, *Nat. Biotechnol.*, 2003, **21**, 1171–1178.
9 S. Kinge, M. Crego-Calama and D. N. Reinhoudt, *ChemPhysChem*, 2008, **9**, 20–42.
10 D. Han, G. Li, J. Wang, T. Zheng, L. Peng, L. Li and T. Jiao, *Colloids Surf.*, 2023, **676**, 132182.
11 B. Yu and M. Meyyappan, *Solid-State Electron.*, 2006, **50**, 536–544.
12 D. Lombardo, P. Calandra, L. Pasqua and S. Magazù, *Materials*, 2020, **13**, 1048.
13 I. S. Costin and G. T. Barnes, *J. Colloid Interface Sci.*, 1975, **51**, 106–121.
14 G. T. Barnes, *Colloids Surf., A*, 2001, **190**, 145–151.
15 E. Bergendal, P. Gutfreund, G. A. Pilkington, R. A. Campbell, P. Müller-Buschbaum, S. A. Holt and M. W. Rutland, *Nanoscale*, 2021, **13**, 371–379.
16 E. Bergendal, R. A. Campbell, G. A. Pilkington, P. Müller-Buschbaum and M. W. Rutland, *Nanoscale Horiz.*, 2020, **5**, 839–846.
17 J. F. D. Liljeblad, E. Tyrode, E. Thormann, A. C. Dublanchet, G. Luengo, C. Magnus Johnson and M. W. Rutland, *Phys. Chem. Chem. Phys.*, 2014, **16**, 17869–17882.
18 K. S. Novoselov, A. K. Geim, S. V. Morozov, D. Jiang, Y. Zhang, S. V. Dubonos, I. V. Grigorieva and A. A. Firsov, *Science*, 1979, **2004**(306), 666–669.
19 A. K. Geim and K. S. Novoselov, *Nat. Mat.*, 2007, **6**, 183–191.
20 K. S. Novoselov, V. I. Fal'Ko, L. Colombo, P. R. Gellert, M. G. Schwab and K. Kim, *Nature*, 2012, **490**, 192–200.
21 A. C. Ferrari, F. Bonaccorso, V. Fal'ko, K. S. Novoselov, S. Roche, P. Bøggild, S. Borini, F. H. L. Koppens, V. Palermo, N. Pugno, J. A. Garrido, R. Sordan, A. Bianco, L. Ballerini, M. Prato, E. Lidorikis, J. Kivioja, C. Marinelli, T. Ryhänen, A. Morpurgo, J. N. Coleman, V. Nicolosi, L. Colombo, A. Fert, M. Garcia-Hernandez, A. Bachtold, G. F. Schneider, F. Guinea, C. Dekker, M. Barbone, Z. Sun, C. Galiotis, A. N. Grigorenko, G. Konstantatos, A. Kis, M. Katsnelson, L. Vandersypen, A. Loiseau, V. Morandi, D. Neumaier, E. Treossi, V. Pellegrini, M. Polini, A. Tredicucci, G. M. Williams, B. Hee Hong, J. H. Ahn, J. Min Kim, H. Zirath, B. J. Van Wees, H. Van Der Zant, L. Occhipinti, A. Di Matteo, I. A. Kinloch, T. Seyller, E. Quesnel, X. Feng, K. Teo, N. Rupesinghe, P. Hakonen, S. R. T. Neil, Q. Tannock, T. Löfwander and J. Kinaret, *Nanoscale*, 2015, **7**, 4598–4810.
22 J. Zhang, H. Peng, H. Zhang, S. Maruyama and L. Lin, *Adv. Funct. Mater.*, 2022, **32**, 2208378.
23 E. Bergendal and M. W. Rutland, *Langmuir*, 2024, **40**, 10468–10476.
24 M. Vázquez Sulleiro, A. Develioglu, R. Quirós-Ovies, L. Martín-Pérez, N. Martín Sabanés, M. L. Gonzalez-Juarez, I. J. Gómez, M. Vera-Hidalgo, V. Sebastián, J. Santamaría, E. Burzurí and E. M. Pérez, *Nat. Chem.*, 2022, **14**, 695–700.

